

Simulated optical molasses cooling of trapped antihydrogen

Spencer J. Walsh,¹ C. Ø. Rasmussen,² and F. Robicheaux^{1,*}

¹*Department of Physics and Astronomy, Purdue University, West Lafayette, Indiana 47907, USA*

²*CERN, Experimental Physics Department, CH-1211 Genève 23, Switzerland*

(Dated: November 13, 2024)

We theoretically and computationally investigate the cooling of antihydrogen, $\bar{\text{H}}$, using optical molasses cooling. This updates the results in Ref. [1] to the current capabilities of the ALPHA experiment. Through Monte Carlo simulation, we show that $\bar{\text{H}}$ s do not give the standard cooling even in an ideal optical molasses because of their small mass and large transition frequency. For optical molasses cooling in the ALPHA trap, the photons are constrained to travel in one direction only. It is only through the phase space mixing in the trap that cooling in all directions can be achieved. We explore the nontrivial role that laser intensity plays in the cooling. We also investigate the possibility for simultaneously cooling atoms in either of the trapped ground states.

I. INTRODUCTION

The antimatter version of the hydrogen atom, $\bar{\text{H}}$, is the simplest atomic antimatter and as such offers several possibilities for high precision comparison with hydrogen atoms. Cold $\bar{\text{H}}$ atoms were magnetically trapped 14 years ago[2] enabling measurements of its properties. Proposed and actual comparisons included the 1S-2S transition frequency,[3, 4] the hyperfine ground state splitting,[5, 6] charge,[7–9] and acceleration from gravity.[10, 11] Other possible measurements (e.g. 1S-3S or 2S- n S or 2S- n P) of sufficient accuracy would constrain the charge radius of the antiproton as has been done for the proton.[12]

The mechanism forming $\bar{\text{H}}$, three body recombination,[13–15] leads to center of mass temperatures comparable to that of the positron plasma. Since the magnetic trap only holds atoms with less than $\sim 1/2$ K energy, the accuracy of measurements are limited by the relatively high $\bar{\text{H}}$ velocities. The need for colder $\bar{\text{H}}$ atoms led to several proposals for different types of laser cooling and a successful implementation of an optical molasses cooling based on the 1S-2P transition.[16]

Whatever differences between normal hydrogen and $\bar{\text{H}}$ atoms exist, they will be small. Thus, different methods used to cool normal hydrogen could serve as possible templates for cooling $\bar{\text{H}}$. [17–24] However, two important constraints eliminates many methods or limits their effectiveness. The first is that collisional type cooling (e.g. evaporative cooling or sympathetic cooling) is unavailable due to the extremely low density ($< 10^3 \text{ cm}^{-3}$) of $\bar{\text{H}}$ in the trap and the annihilation of $\bar{\text{H}}$ on normal matter. The second constraint derives from the geometry of the trap and the sources of the magnetic fields reducing the effectiveness of laser cooling techniques. For example, the coils that shape the magnetic fields limit the spatial dependence of the magnetic field to relatively smooth variations. Another example is the laser access leads to

a small number of laser beams most constrained to near the axis of the trap.

The most promising cooling technique, and the only one successfully implemented, is a simple optical molasses based on the 1S-2P transition. For this case, a single 121.6 nm beam, somewhat red detuned from the transition in the magnetic field, cools the axial motion of the $\bar{\text{H}}$ atoms. For this geometry, the random re-emission of the photon tends to heat the radial motion. Because the magnetic trapping potentials are not perfectly symmetric, the $\bar{\text{H}}$ motion mixes the axial and radial degrees of freedom[25, 26] which can lead to cooling of all 3 directions.[1, 16] The intensity of the laser has to be sufficiently low that there is time for the mixing to take place between successive photon scattering otherwise the atoms will heat on average. This heating is strongest for smallest detuning where the photon scattering rate is largest. The spatially varying magnetic field also complicates the photoabsorption by giving substantial changes in the detuning versus position in the trap.

There are three main updates to Ref. [1]. First, we recognize that some of the changes from optimal detuning are due to the small mass and large frequency of the cooling transition (Sec. III). Second, we use magnetic fields and laser parameters more representative of the ALPHA experiment (Sec. IV) leading to lower simulated temperatures. Lastly, we describe a possible method for simultaneously laser cooling the 1Sc and 1Sd trapped populations (Sec. V) leading to an important improvement to precision measurements.

In this manuscript, we revisit the simple optical molasses for hydrogen atoms because the large frequency of the 1S-2P transition and small atom mass leads to non-standard results. We describe the Monte Carlo simulation of the optical molasses cooling in the ALPHA trap. We describe why cooling both trapped populations is not possible for a single frequency but can be accomplished for 2 or more frequencies. We give results that indicate the role played by detuning and the intensity.

* robichf@purdue.edu

II. ENERGY LEVELS IN MAGNETIC FIELD

In the ALPHA experiment, $\bar{\text{H}}$ s are laser cooled in a magnetic trap with a minimum $B \sim 1$ T[16]. This means the energy levels are strongly changed from their low (or zero) field character. Reference [27] discusses the energy levels. The energies in a magnetic field are labeled with a Roman letter at the end which, by convention, increases from low to high energy for 1S states while increasing from high to low energy for the 2P states (as ordered for small B). There are two 1S states that can be trapped called the 1Sc and 1Sd states. The 1Sd state has the positron and antiproton spin aligned; in the 1Sc state, they are antiparallel. To prevent losses from the photon emission step, the laser will excite the 2Pa state which has the positron spin and orbital angular momentum aligned to give total positron angular momentum $J = 3/2, M = 3/2$. Because of the different magnetic moments, the transition frequency for the 1Sc-2Pa transition is approximately 675 MHz higher than that for the 1Sd-2Pa transition at 1 T. The difference in frequencies does not change much with increasing B ; for example, at $B = 0.5$ T, the difference in frequencies is 660 MHz while the difference in frequencies is 680 MHz at 1.5 T.

The hyperfine splitting of the 2P states is several 10's MHz compared to the order 10 GHz splitting of the states. Thus, the antiproton spin is nearly decoupled from the positron total angular momentum, J , at the ~ 1 T of the ALPHA experiment. The 1Sd-2Pa transition is exactly closed because all of the angular momenta are aligned. The 1Sc-2Pa transition is not exactly closed because the 1S state, with a more than 10 \times larger hyperfine splitting than 2P, has more mixing of the wrong direction antiproton spin. After the 1Sc-2Pa transition, the 2Pa state decays to the 1Sa state with a branching ratio from perturbation theory of

$$\mathcal{B} = \left(\frac{1.42 \text{ GHz}}{4 \times 14.0 \text{ (GHz/T)} \times B} \right)^2 \quad (1)$$

where the numerator is from the 1S hyperfine splitting and the denominator is from the Zeeman splitting when flipping the positron spin. For $B \sim 1$ T, the branching ratio is $\sim 6.4 \times 10^{-4}$. Thus, the cooling of the 1Sc population in the ALPHA trap should use less than ~ 100 photons to lose less than 10% of the population to spin flip. The $\bar{\text{H}}$ can be cooled to steady state with less than ~ 100 photons so the spin flip is not a problem as long as the cooling is not overextended. For smaller B , the spin flip losses are larger and could become a serious issue below ~ 0.1 T.

III. MONTE CARLO: NO MAGNETIC TRAP

As discussed in the introduction, laser cooling of trapped $\bar{\text{H}}$ is complicated by the changing transition frequency due to the motion through the spatially varying

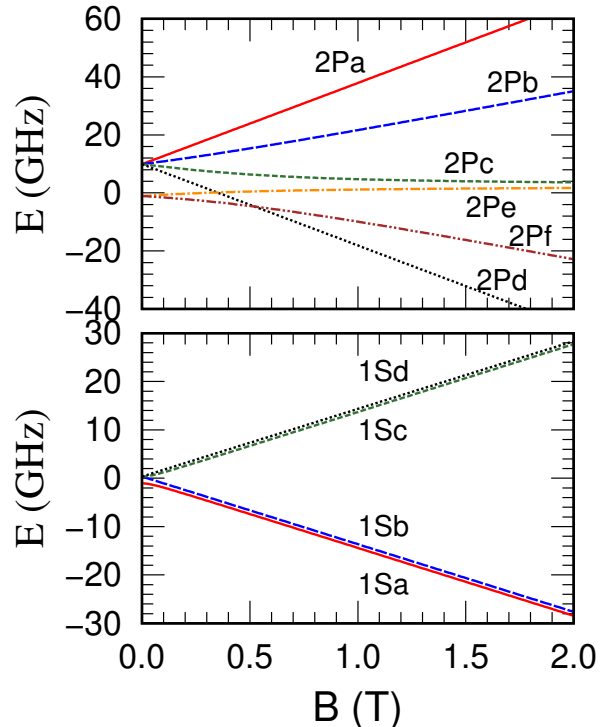


Figure 1. The splittings of the 1S and 2P states relative to their zero field average. The hyperfine terms of the 2P states are too small to resolve.

B -field. The cooling is also complicated by the fact that the photons only travel in one direction and thus can only cool one component of the velocity. Cooling of all directions relies on the motion through the trap to mix the velocity components. To help with understanding the changes to optical molasses cooling due to the special circumstances of the ALPHA trap, we present in this section results when the restrictions of the trap are removed. Section III A reminds the reader of a small energy shift in the laser tuning that arises from the small mass and large transition frequency for $\bar{\text{H}}$. Section III B describes an algorithm for laser cooling similar in form to that used in the theory of the actual trap but idealizes the physics by having fast mixing of the velocities and neglecting the frequency shift with position; because of the small mass and large transition frequency, this treatment does not lead to the standard optical molasses temperature versus detuning.

A. Energy shift

A well known recoil term is usually left out in descriptions of laser cooling, due to its smallness in determining the energy conservation of the transition. For $\bar{\text{H}}$ cooling, this term is large enough that it could cause some changes in the results. Consider the energy before and

after the photon absorption

$$E_g + \frac{1}{2}Mv^2 + \hbar\omega = E_e + \frac{1}{2}M|\vec{v} + \vec{v}_k|^2 \quad (2)$$

where $E_{e,g}$ are the internal excited, ground state energies, M is the mass of the atom, \vec{v} is the atom velocity before the photon absorption, $f = \omega/(2\pi)$ is the frequency of the photon, and $\vec{v}_k = \hbar\vec{k}/M$ is the recoil velocity from the photon absorption with k the photon wave number. Solving for ω gives the resonance condition[28]

$$\omega_r(\vec{v}) = \frac{E_e - E_g}{\hbar} + \vec{v} \cdot \vec{k} + \frac{\hbar k^2}{2M} = \omega_0 + \vec{v} \cdot \vec{k} + \frac{\hbar k^2}{2M} \quad (3)$$

with $\omega_0/(2\pi)$ the nominal resonance frequency, $\vec{v} \cdot \vec{k}$ is from the Doppler effect, and the last term is a recoil contribution to the energy.

Typically, the last term is dropped because it is much smaller than the linewidth or other interesting energy scales. For $\bar{\text{H}}$, this term corresponds to a frequency of 13.4 MHz, approximately 13% of the linewidth. In all that follows, we will consider this term to be added to the ω_0 .

B. Ideal Optical Molasses

In this section, we describe a method for Monte Carlo simulations of laser cooling of $\bar{\text{H}}$ using an ideal optical molasses[29]. We use a method similar to Sec. IV but is idealized by having the velocity mix much faster than the times between photon scattering and by not including the shift in detuning as the $\bar{\text{H}}$ moves through the trap. Ideal optical molasses cooling assumes the photon has a wave vector, \vec{k} , in a random direction relative to the atom's velocity, \vec{v} . The Doppler effect leads to an effective detuning of

$$\Delta = \omega - \omega_r(\vec{v}) = \Delta_0 - \vec{k} \cdot \vec{v} \quad (4)$$

where $\Delta_0 = 2\pi\delta f$ with δf the frequency detuning of the laser in the lab frame including the shift described in the previous section. A negative detuning leads to more absorption when the atom's velocity is opposite to the photon propagation direction resulting in a kick from the absorption step tending to slow the atom. For the ideal optical molasses, we will take the photon emission to be in a random direction which leads to heating on average. After one absorption and emission event, the velocity changes by

$$\vec{v} \rightarrow \vec{v} + \frac{\hbar\vec{k}}{M} - \frac{\hbar\vec{k}_{emit}}{M}. \quad (5)$$

When $\hbar k/M$ is small compared to the atom speed, then the ideal optical molasses leads to the lowest average atom kinetic energies when $\Delta_0 = -\Gamma/2$ with Γ the decay rate of the excited state. For this detuning, the minimum average energy is $\langle E \rangle_{\min} = 3\hbar\Gamma/4$ corresponding to

$k_B T_{\min} = \hbar\Gamma/2$ where k_B is Boltzmann's constant[29]. For general detuning, the ideal optical molasses gives a steady state temperature[29]

$$k_B T_{\text{om}} = -\frac{\hbar\Gamma}{4} \left[1 + \left(\frac{2\Delta_0}{\Gamma} \right)^2 \right] \frac{\Gamma}{2\Delta_0} \quad (6)$$

where we have assumed the Rabi frequency of the transition, Ω , is much smaller than Γ so that power broadening can be ignored.

Our Monte Carlo simulation of the ideal optical molasses used the following algorithm: (1) for each of N atoms, randomize the direction of the atom's velocity, \vec{v} , and for that atom compute the effective detuning, Eq. (4); (2) compute the probability that the photon was absorbed using $P = P_0/[1 + (2\Delta/\Gamma)^2]$ with P_0 a small number of order 0.01; (3) compute a random number; if it is smaller than P , then a photon was absorbed; (4) if a photon is absorbed, compute a random emission direction and use Eq. (5) to update that atom's velocity. If we wanted to simulate the effect of thermalization from elastic collisions between the atoms, we added a step: (5) randomly pick pairs of atoms and rotate their relative velocity to emulate a collision; repeated often enough step (5) leads to a Maxwell-Boltzmann velocity distribution at temperature $k_B T = (2/3)\langle KE \rangle$.

For $\bar{\text{H}}$ cooled on the $1S - 2P$ transition, $k \simeq 2\pi/121.6$ nm, $\Gamma \simeq 6.26 \times 10^8$ s⁻¹, and M is the hydrogen atom mass. The recoil velocity $\hbar k/M \simeq 3.26$ m/s and the recoil energy $\hbar^2 k^2/2M \simeq 8.87 \times 10^{-27}$ J $\simeq 0.642$ mK k_B . For an ideal optical molasses, the expected lowest temperature is $T_{\min} \simeq 2.39$ mK for detuning $\Delta_0 = -\Gamma/2$.

The results of the simulations are shown in Fig. 2. Figure 2(a) shows the results of the simulations when we did not include collisions between the atoms, skipping step (5) of the algorithm. This figure shows the results when the photon wavelength is kept at 121.6 nm but we artificially change the mass of the $\bar{\text{H}}$ from 1 to 16 times the actual mass by factors of 2 in order to illustrate the role that the small atomic mass plays in the change of the steady state temperature from the ideal result of Eq. (6). The blue long-dash curve is for the actual $\bar{\text{H}}$ mass. The red solid curve is the ideal case, Eq. (6).

The minimum temperature that can be reached for $1M$ happens for a detuning of $\Delta_0 \simeq -1.1\Gamma$ and gives $T \simeq 3.05$ mK. The temperature for $1M$ at $\Delta_0 = -\Gamma/2$ (the minimum of Eq. (6)) is $\simeq 19$ mK which is almost $8\times$ hotter than expected from the usual optical molasses relations. From Fig. 2(a), the higher masses become progressively closer to the ideal optical molasses case, red solid line. The reason for the discrepancy is the large size of the velocity kick, 3.26 m/s, compared to the thermal speed $\sqrt{k_B T/M} \sim 4.4$ m/s at 2.39 mK (the minimum for the ideal optical molasses). Interestingly, the $1M$ temperature is less than the ideal case by ~ 0.9 mK for larger magnitude detunings, $\Delta_0 < -\Gamma$.

In the antihydrogen traps, the $\bar{\text{H}}$ density is too low for elastic collisions to play a role in thermalizing the

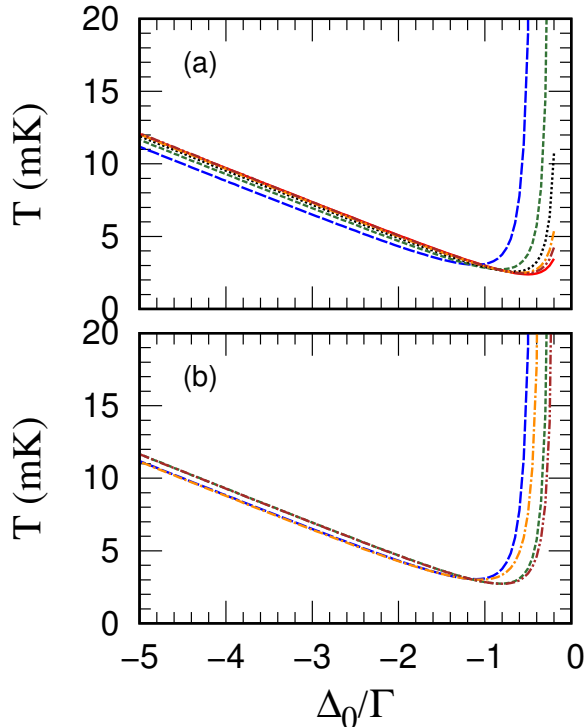


Figure 2. For an ideal optical molasses, the steady state temperature using the Monte Carlo method versus the lab frame detuning in units of Γ . For (a), there is no collision between the atoms to achieve a Maxwell-Boltzmann velocity distribution. The different lines are for different \bar{H} masses to illustrate the role that the small atomic mass plays in the steady state temperature: blue long dash ($1M$), green dash ($2M$), black dot ($4M$), orange dash-dot ($8M$), maroon dash-dot-dot ($16M$), and red solid is the ideal case, Eq. (6). For (b), we compare the effect that elastic collisions leading to thermalization has on the steady state temperature: no collisions [blue long dash ($1M$), green dash ($2M$)], with collisions [orange dash-dot ($1M$), maroon dash-dot-dot ($2M$)].

distribution. However, in other atomic experiments of hydrogen, the density might be high enough for elastic collisions to play a role. In Fig. 2(b), we show the results of laser cooling while including elastic collisions between the atoms to give a Maxwell-Boltzmann distribution. We show the results without (blue long dash and green dash curves) and with (orange dash-dot and maroon dash-dot-dot) elastic collisions. The collisions allow for lower temperatures for $1M$ and $2M$. The difference arises because the no collision case leads to a few atoms with quite high kinetic energy. The collisions bring them back to lower speeds where they can be more efficiently cooled.

IV. MONTE CARLO: ANTIHYDROGEN TRAP

The Monte Carlo simulation of cooling in the ALPHA trap is more complicated than the algorithm in the pre-

vious section because the atoms are confined to move in a magnetic trap. Our simulations are similar to those in Ref. [1] but with details updated for the current ALPHA trap. Also, see Ref. [27] for an overview for how the \bar{H} s are trapped and probed.

Some of the features specific for the optical molasses cooling include the path of the laser which is a straight line with a 2.3° tilt relative to the trap axis taken to be the z -direction. Thus, the \vec{k} is a constant. The motion of the \bar{H} through the trap mixes the different velocity components possibly allowing for three dimensional cooling. Since this mixing is relatively slow, the detuning and intensity need to be chosen to limit the heating of the radial motion due the photon emission step. The beam has a waist of 3.48 mm. On the trap axis, $B_\perp/B_z < 0.0003$ while at a radius of 5 mm the $B_\perp/B_z < 0.05$ which means the direction of \vec{B} has little effect. The laser is pulsed with a duration of 10's of nanoseconds and with repetition rate of 50 Hz. The laser cooling happens over a time scale measured in hours which is possible due to the cryogenic vacuum.

Because the atoms are in a large B -field, only one of the two trapped states can be cooled if the laser frequency is held fixed. To give an idea, the $1Sc$ - $2Pa$ transition at $B = 1$ T is approximately 675 MHz higher frequency than the $1Sd$ - $2Pa$ while the linewidth is approximately 100 MHz. If the laser is set to cool the $1Sd$ \bar{H} s, then there is almost no photons scattered by atoms in the $1Sc$ state. While if the $1Sc$ \bar{H} s are cooled, the $1Sd$ \bar{H} s will be heated because the laser will be blue detuned relative to this transition. A possible method for cooling both trapped states to the same extent is discussed in Sec. V.

Because the emission is from an $\ell = 1, |m| = 1$ state to an $\ell = 0$ state, the probability for emission into different directions is not uniform. If θ is the angle between the B -field direction and the photon emission direction, the probability for photon emission into a solid angle $d\phi d(\cos \theta)$ is proportional to $1 + \cos^2 \theta$. This somewhat suppresses the emission perpendicular to \vec{B} relative to an isotropic distribution. Suppressing perpendicular emission helps with cooling in the ALPHA trap because heating of the perpendicular directions due to photon emission is one of the limiting factors.

One of the important features is that the detuning of the photon depends on the position in the trap as well as the Doppler shift. The reason for this is the B -field changes with position in the trap and the $1S - 2P$ resonance frequency increases with increasing B -field. For negative detuning, the detuning becomes increasingly negative with increasing B -field. Figure 3 shows the magnitude of the B -field on the trap axis as a function of the position on the axis relative to the trap center. There are 5 mirror coils and 2 solenoidal coils that are used to shape the B -field on the axis. The red solid line is a flat field similar to that used in the $1S2S$ spectroscopy measurements in Ref. [4]. The blue long dash line gives a more harmonic trap used in some of the simulations below. The green dashed and black dot curves are the

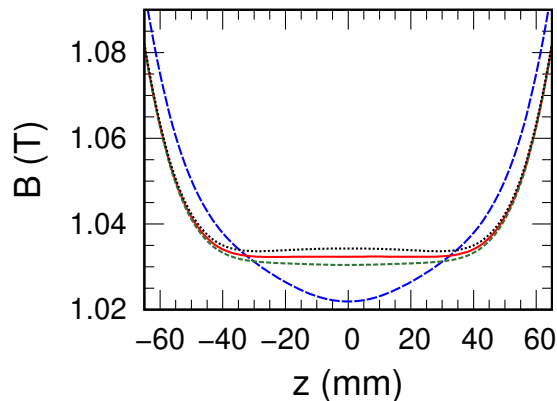


Figure 3. The magnetic fields for the four simulations described in the text. The red solid line is the “flat” B -field, Sec. IV A and the blue long dash line is the “harmonic” B -field, Sec. IV C. The green dashed and black dot curves are the slightly dipped and raised traps of Secs. IV B. The z is the distance from the trap center along the trap axis.

slightly dipped and raised traps of Sec. IV B.

The B -field scale can be converted to an energy scale by using the magnetic moment for the $1S$ state which is approximately $2/3$ K/T. This means that a 0.03 T change in B -field is a 20 mK k_B change in potential energy. The change in the detuning is approximately -14 MHz/mT. Thus, a 0.03 T increase in B -field gives a 420 MHz more negative detuning.

The laser line width, estimated as 60 MHz full-width half-maximum (FWHM), also modestly affects the results since the intrinsic linewidth is approximately 100 MHz. The laser line width is incorporated into the simulation by having each pulse at a slightly different detuning randomly chosen from a Gaussian distribution with a FWHM of 60 MHz. This leads to an effectively broader transition although the effect is not large. We verified that this is a very good approximation (errors less than a couple percent) by comparing to the results from numerically solving the Optical Bloch equations for the same parameters. In all of the figures and results, the linewidth, Γ , is the natural radiative linewidth of the $2P$ state.

Reference [1] investigated the cooling from a hot distribution. This requires a large amount of time to reach steady state because many of the trajectories only rarely cross the laser beam. One can use a short cut by starting with cold initial conditions and letting the atoms come to a steady state. This allows a much faster determination of the steady state. We launched the \bar{H} s from a small region in the center of the trap with a thermal velocity distribution so the average initial energy is similar to the final, steady state energy. We ran the trajectories for either 1 or $3/2$ simulation hours in the laser to ensure a steady state was achieved.

Because the laser is approximately on the axis, it is possible that the laser cools the axial motion but heats

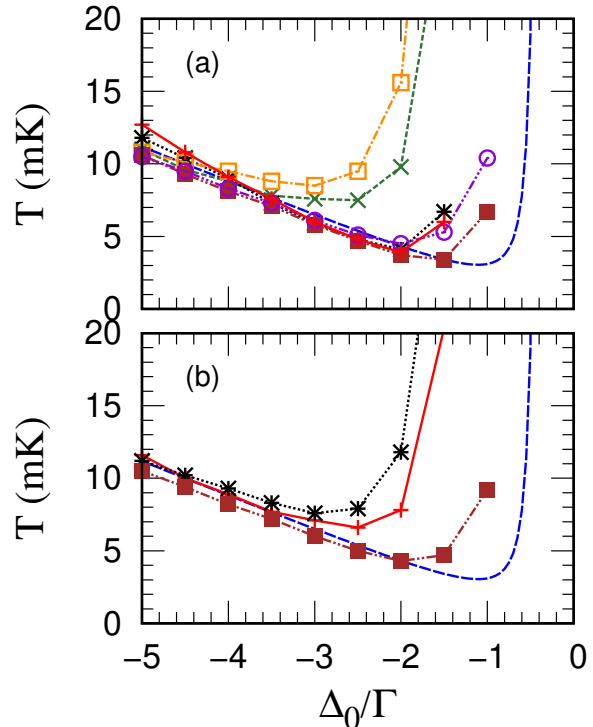


Figure 4. Comparison of steady state temperatures versus detuning for different pulse energy. The calculations were done for the flat field of Fig. 3. In both (a) and (b), the blue long dash is the same as the $1M$ in Fig. 2. For (a) the curves are: red solid (+) T_z for 1 nJ, green dash (\times) T_r for 1 nJ, black dot (*) T_z for 2 nJ, orange dash-dot (open square) T_r for 2 nJ, maroon dash-dot-dot (solid square) T_z for 2 nJ with artificial mixing, and purple dash-dot-dot-dot (open circle) T_r for 2 nJ with artificial mixing. For (b) the curves are: red solid (+) $T = (2T_r + T_z)/3$ for 1 nJ, black dot (*) T for 2 nJ, and maroon dash-dot-dot (solid square) T for 2 nJ with artificial mixing.

up (or doesn’t cool as well) the radial motion. After the \bar{H} s reach steady state, we compute the averages $T_z \equiv 2\langle KE_z \rangle / k_B$ and $T_r \equiv \langle KE_z + KE_y \rangle / k_B$ while the laser is on. We also calculate the average energy of the \bar{H} s. In the flat field, the average energy is approximately $2k_B T$ for thermal distributions with $T < \sim 50$ mK.

A. Cooling in a flat field

Figure 4 compares the steady state temperatures for two different laser energies per pulse: 1 nJ or 2 nJ. These calculations were done for the flat field in Fig. 3. For comparison, the ideal case for $1M$ from Fig. 1 is included as the blue long dash line. Both the T_z and T_r are shown in (a) while the combination $T = (2T_r + T_z)/3$ is shown in (b). At larger detuning, all of the temperatures are approximately that for the ideal optical molasses for $1M$. However at smaller detuning, the temperatures in the

trap tend to be higher than the ideal case with $T_r > T_z$. Also, the T_r is larger for the 2 nJ pulses than for the 1 nJ pulses. As the magnitude of the detuning decreases, this effect becomes larger and is notable for $|\Delta_0| < 3\Gamma$. This indicates that the coordinate mixing by the \bar{H} motion through the trap is too slow to keep up with the cooling in z and heating in r . The rate for scattering photons increases as the $|\Delta_0|$ decreases. Roughly speaking, the mixing in the trap can keep up with the cooling of z and heating in r for $|\Delta_0| > 3.5\Gamma$ but can't for smaller detuning. Also, the mixing rate decreases as the axial motion is cooled which can lead to radial heating if the axial cooling is too fast. Because more photons are scattered with 2 nJ pulses, the effect is larger for the larger intensity.

For a clearer picture of this effect, we repeated the simulation but added artificial mixing into the coordinates. This was done by randomly making small changes to the direction of the \bar{H} velocity. We chose parameters so that $\langle \vec{v}(t) \cdot \vec{v}(0) \rangle = v^2(0)e^{-t/T}$ with $T = 50$ s when there are no trapping forces. These are the artificial mixing curves in Fig. 4 which are at much lower temperature and more closely track the ideal molasses case at small $|\Delta_0|$. In Ref. [1], the lowest average energy in Table 2 was 32 mK which corresponds to a temperature of ~ 16 mK. This result is substantially hotter than Fig. 4 because substantially higher energy laser pulses were used: 50 nJ with 10 Hz repetition rate and circular polarization. The current simulations with 2 nJ at 50 Hz repetition rate and linear polarization is effectively $10\times$ fewer photons per second. This is also why the simulations in Ref. [1] were for only a couple 100 seconds while the current simulations are for 1000's of seconds.

B. Cooling in a slightly dipped or raised field

We simulated cooling when the middle mirror coil is used to generate a dip in the magnetic trap, Fig. 3 green dash curve. This leads to a clear minimum of ~ 2 mT compared to the flat field. On an energy scale, this corresponds to $\sim 4/3$ mK k_B which is much smaller than the scale in Fig. 4. We also simulated a small hump by changing the current in the middle mirror, Fig. 3 black dot curve, with a clear maximum of ~ 2 mT compared to the flat field. Because these are small changes in energy compared to the temperatures in Fig. 4, it might be expected that the results will not be much different from the previous section.

Similar to a result in Ref. [1], we found that the \bar{H} coldest temperature was a bit higher than in the flat trap for the slightly dipped field. The \bar{H} coldest temperature was approximately 10% higher than in the previous section. We also found the \bar{H} coldest temperature was a bit lower than in the flat trap for the slightly raised field. In these two cases, the T_z was hardly changed from that for the flat field. The changes were in the T_r and reflect the longer or shorter mixing times of the trajectories in the dipped or raised field.

C. Cooling in a nearly harmonic trap

The harmonic trap, blue long dash curve in Fig. 3, has only a tiny region where the detuning has smallest magnitude. This suggests that the problems with the photon scattering rate being higher than the coordinate mixing rate will be less. The actual case is that the harmonic trap has much smaller mixing rate between the coordinates. We find that the temperature differences are much more extreme than the previous section. For example, at $\Delta_0 = -3\Gamma$ and 2 nJ, $T_z \simeq 6$ mK and $T_r \simeq 24$ mK for the harmonic trap while the flat trap has $\simeq 6$ and $\simeq 9$ mK. Thus, nearly harmonic traps appear to be a poor choice for laser cooling of only the axial motion. Similarly, making a much larger hump in the previous section also leads to less effective cooling because the two side wells become more harmonic like.

V. SIMULTANEOUS COOLING 1Sc AND 1Sd

Because magnetic fields in the ALPHA experiment slowly drift with time, measurements that require both trapped states (e.g. Ref. [6]) requires simultaneous measurements of the 1Sc and 1Sd trapped populations for high accuracy. This is straightforward when measurements are performed on uncooled populations. There are no mechanisms to distinguish the formation of antiproton up versus down states which is the main difference between 1Sc and 1Sd.

Unfortunately, problems arise when laser cooling both populations and trying to achieve the same distributions for each. The 1Sc-2Pa transition frequency is 675 MHz larger at $B \sim 1$ T than the 1Sd-2Pa. Detuning to -250 MHz for the 1Sd-2Pa transition gives -925 MHz detuning for the 1Sc-2Pa transition. Thus, the cooling is extremely slow for the 1Sc states and the final distribution is at a substantially larger temperature with, essentially, uncooled \bar{H} s.[16] In principle, the 1Sc and 1Sd states could be mixed using microwaves with frequencies less than 1 GHz, but such long wavelength light does not propagate down the ~ 22 mm radius ALPHA trap; this would require a special resonator and microwave input in the next generation trap.

One possibility that would lead to nearly the same distributions would use (say) -250 MHz detuned for the 1Sd-2Pa transition (-925 MHz detuning for 1Sc-2Pa), then 675 MHz higher than this (425 MHz detuning for 1Sd and -250 MHz detuning for 1Sc), and then 675 MHz higher (1100 MHz detuning for 1Sd and 425 MHz detuning for 1Sc). If these frequencies are interleaved, the very far off resonance photons (1100 MHz for 1Sd and -925 MHz for 1Sc) would contribute almost no cooling or heating. The idea is to use only the lowest frequency until the 1Sd \bar{H} s reached a steady state. Then the laser pulses would alternate between f or $f + 675$ MHz. After the 1Sc are also cooled, then the frequencies would cycle f then $f + 675$ then $f + 1350$ MHz (repeat) so both

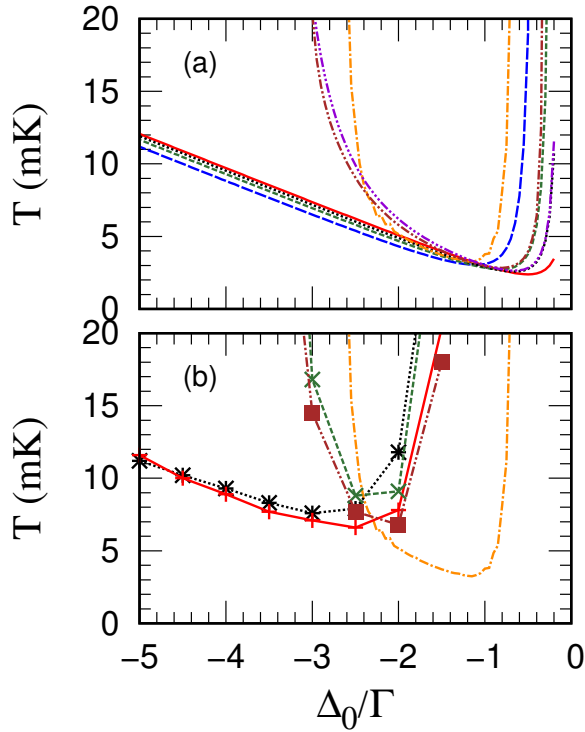


Figure 5. (a) is similar to Fig. 2(a). Four curves are from this figure where the ideal one frequency optical molasses cools $\bar{\text{H}}$ s with different masses to a steady state temperature: blue long dash ($1M$), green dash ($2M$), black dot ($4M$), and red solid is the ideal case, Eq. (6). Three of the curves use the two frequency cooling where every other photon pulse has detuning Δ_0 or $\Delta_0 + 2\pi 675$ MHz. The curves are: orange dash-dot ($1M$), maroon dash-dot-dot ($2M$), purple dash-dot-dot-dot ($4M$). (b) The orange dash-dot is the same from (a) while the black dot (*) is $T = (2T_r + T_z)/3$ from the constant full simulation in the ALPHA trap with 2 nJ pulses, Fig. 4(b). The green dash (x) is the two frequency results for 2 nJ and the maroon dash-dot-dot (solid square) is the two frequency results for 1 nJ.

populations experience the same cooling. This method would work if interleaving (say) -250 MHz detuning with 425 MHz detuning leads to steady state cold atoms in the 1Sd state.

Before treating the cooling in the ALPHA trap, we examine the stability of the ideal optical molasses with two frequencies. Figure 5(a) shows the steady state temperature for ideal optical molasses for 3 different $\bar{\text{H}}$ masses: $1M$, $2M$, and $4M$. Three of the curves are when there is only one frequency and are the same as Fig. 2(a): blue long dash ($1M$), green dash ($2M$), and black dot ($4M$). The red curve is the ideal optical molasses, Eq. (6). Three of the curves are the steady state temperature when two frequencies are used: orange dash-dot ($1M$), maroon dash-dot-dot ($2M$), and purple dash-dot-dot-dot ($4M$). We first ran at detuning Δ_0 until a steady state was reached. Then the laser pulses alter-

nated between Δ_0 and $\Delta_0 + 2\pi 675$ MHz. As expected, alternating with a blue detuned pulse leads to hotter steady states. The $2M$ and $4M$ cases behave more as we were expecting: the smaller $|\Delta_0|$ being less affected by the blue detuned photons. The $1M$ case does not behave in quite the same way. Probably this is because smaller $|\Delta_0|$ leads to stronger heating for $1M$ (see the blue long dash curve). The hotter $\bar{\text{H}}$ s interact more strongly with the blue detuned pulses which increases their temperature further. Despite this, the orange dash-dot curve has a region $-2\Gamma < \Delta_0 < -\Gamma$ of nearly unchanged cooling. Comparing this region to the steady state temperatures in Fig. 4(b), suggests that two frequency cooling might work in the ALPHA trap.

The results from simulations in the trap are shown in Fig. 5(b) as the green dash (x) for 2 nJ pulses and maroon dash-dot-dot-dot (solid square) for 1 nJ pulses. There appears to be a small range of detuning (roughly $-3\Gamma < -\Delta_0 < -2\Gamma$) that leads to decent cooling even with the heating from the blue detuned frequency. This range is narrow because the cooling in the trap without the blue detuned pulses is not good for $-2\Gamma < \Delta_0$ and the blue pulses lead to heating for $\Delta_0 < -3\Gamma$. The two detunings -2.5 and -2Γ have nearly the same temperature as the one frequency case (these are the black dot (*) and red solid (+) curves). The simulations are somewhat unrealistic in that the frequency was held constant for 1 second before switching to a different frequency. In practice, the frequencies probably can not be switched that often. However, it is only necessary to change the frequencies on a time scale where a small number of photons are scattered before the change. Depending on the trap and laser details, probably this would be on the several minute scale. These simulations suggest that the 1Sc and 1Sd states can be simultaneously cooled in the ALPHA trap.

VI. SUMMARY

Laser cooling of $\bar{\text{H}}$ s has been demonstrated in Ref. [16]. We have updated the laser cooling results of Ref. [1] to better reflect the parameters of the ALPHA experiment. The update includes laser parameters and magnetic field simulation.

Simulations show that even ideal optical molasses is complicated for $\bar{\text{H}}$ s. For ideal optical molasses, the optimum detuning is $\Delta_0 = -\Gamma/2$ leading to a minimum temperature of $k_b T = \hbar\Gamma/2$ where Γ is the decay rate of the upper state. Because $\bar{\text{H}}$ s are cooled on the $1S - 2P$ transition, the small mass and large photon energy leads to relatively large recoil velocity and energy. For untrapped $\bar{\text{H}}$ s, we find that the optimum detuning is $\Delta_0 \simeq -1.1\Gamma$ with a minimum temperature of $k_b T \simeq 1.28\hbar\Gamma/2$; a detuning $\Delta_0 = -\Gamma/2$ leads to a temperature $k_b T \sim 8 \times \hbar\Gamma/2$.

The spatially varying magnetic fields of the ALPHA trap adds a complication to the cooling due to the con-

strained geometry for the laser. Three dimensional cooling relies on the atom motion to scramble the velocity vector. For perfectly separable motion in x, y, z , the atoms could not be cooled. Larger energy per laser pulse leads to a higher photon scattering rate which means the atoms' motion along the laser can be cooled faster. However, the limits of velocity mixing means that larger energy per pulse can lead to higher steady state temperature. Larger energy per laser pulse requires larger magnitude detuning to reach lower temperatures. For the cases simulated, the lowest temperatures were achieved with a detuning $\Delta_0 \sim -2.5\Gamma$. We also simulated different shapes for the magnetic trap which can affect the final temperature.

We also simulated the possibility for simultaneously cooling the 1Sd and 1Sc populations. The large magnetic field of the ALPHA trap leads to a 675 MHz detuning between the transitions starting in the 1Sd and the 1Sc states. By interleaving three frequencies in the laser pulses, we found a small region of detuning where both populations can be cooled to the ~ 10 mK regime.

Although we have not simulated the following modifications, the outcomes seem to follow from the results presented above. One possible modification would be to increase the angle of the laser with respect to the trap

axis. While this is not possible in the current ALPHA experiment, a larger angle (say between $20\text{-}40^\circ$) would directly cool two of the spatial coordinates (for example, x and z) and only require mixing of the coordinate perpendicular to the plane defined by the laser and the trap axis. Another possibility is to use stronger laser pulses with larger detuning early in the cooling cycle and then transition to weaker pulses and smaller detuning near the end of cooling; this should lead to faster cooling at early times and lower temperatures at later times.

Data plotted in the figures is available at [30].

ACKNOWLEDGMENTS

FR thanks Claudio Lenz Cesar and AbdAlGhaffar K. Amer for insightful conversations. A portion of the manuscript was written while FR was supported at ITAMP. This work was supported by the U.S. National Science Foundation under Grant No. 2409162-PHY and through a grant for ITAMP at Harvard University. The calculations were performed on a cluster run by the Department of Physics and Astronomy, Purdue University.

-
- [1] P. H. Donnan, M. C. Fujiwara, and F. Robicheaux, "A proposal for laser cooling antihydrogen atoms," *J. Phys. B* **46**, 025302 (2013).
 - [2] G.B. Andresen et al (ALPHA collaboration), "Trapped antihydrogen," *Nature* **468**, 673 (2010).
 - [3] M. Ahmadi et al (ALPHA collaboration), "Observation of the 1s–2s transition in trapped antihydrogen," *Nature* **541**, 506 (2017).
 - [4] M Ahmadi et al (ALPHA collaboration), "Characterization of the 1s–2s transition in antihydrogen," *Nature* **557**, 71 (2018).
 - [5] C. Amole et al (ALPHA collaboration), "Resonant quantum transitions in trapped antihydrogen atoms," *Nature* **483**, 439 (2012).
 - [6] M. Ahmadi et al (ALPHA collaboration), "Observation of the hyperfine spectrum of antihydrogen," *Nature* **548**, 66 (2017).
 - [7] C. Amole et al (ALPHA collaboration), "An experimental limit on the charge of antihydrogen," *Nature Comm.* **5**, 3955 (2014).
 - [8] M. Baquero-Ruiz, A.E. Charman, J. Fajans, A. Little, A. Povilus, F. Robicheaux, J.S. Wurtele, and A.I. Zhmoginov, "Using stochastic acceleration to place experimental limits on the charge of antihydrogen," *New J. Phys.* **16**, 083013 (2014).
 - [9] M. Ahmadi et al (ALPHA collaboration), "An improved limit on the charge of antihydrogen from stochastic acceleration," *Nature* **529**, 373 (2016).
 - [10] P. Hamilton, A. Zhmoginov, F. Robicheaux, J. Fajans, J. S Wurtele, and H. Müller, "Antimatter interferometry for gravity measurements," *Phys. Rev. Lett.* **112**, 121102 (2014).
 - [11] E.K. Anderson et al (ALPHA collaboration), "Observation of the effect of gravity on the motion of antimatter," *Nature* **621**, 716 (2023).
 - [12] R. Pohl et al, "The size of the proton," *Nature* **466**, 213 (2010).
 - [13] F. Robicheaux and J. D. Hanson, "Three-body recombination for protons moving in a strong magnetic field," *Phys. Rev. A* **69**, 010701 (2004).
 - [14] M. E. Glinsky and T. M. O'Neil, "Guiding center atoms: Three-body recombination in a strongly magnetized plasma," *Phys. Fluids B* **3**, 1279 (1991).
 - [15] P. Mansbach and J. Keck, "Monte carlo trajectory calculations of atomic excitation and ionization by thermal electrons," *Phys. Rev.* **181**, 275 (1969).
 - [16] CJ Baker et al (ALPHA collaboration), "Laser cooling of antihydrogen atoms," *Nature* **592**, 35 (2021).
 - [17] ID Setija, HGC Werij, OJ Luiten, MW Reynolds, TW Hijmans, and JTM Walraven, "Optical cooling of atomic hydrogen in a magnetic trap," *Phys. Rev. Lett.* **70**, 2257 (1993).
 - [18] C. L. Cesar, D. G. Fried, T. C. Killian, A. D. Polcyn, J. C. Sandberg, A. Yu Ite, T. J. Greytak, D. Kleppner, and J. M. Doyle, "Two-photon spectroscopy of trapped atomic hydrogen," *Phys. Rev. Lett.* **77**, 255 (1996).
 - [19] V. Zehnlé and J. C. Garreau, "Continuous-wave doppler cooling of hydrogen atoms with two-photon transitions," *Phys. Rev. A* **63**, 021402 (2001).
 - [20] D. Kielpinski, "Laser cooling of atoms and molecules with ultrafast pulses," *Phys. Rev. A* **73**, 063407 (2006).
 - [21] S. Wu, R. C. Brown, W. D. Phillips, and J.V. Porto, "Pulsed sisyphus scheme for laser cooling of atomic (anti) hydrogen," *Phys. Rev. Lett.* **106**, 213001 (2011).

- [22] JM Michan, MC Fujiwara, and T Momose, “Development of a Lyman- α laser system for spectroscopy and laser cooling of antihydrogen,” *Hyperfine Interactions* **228**, 77 (2014).
- [23] J. M. Michan, G. Polovy, K. W. Madison, M. C. Fujiwara, and T. Momose, “Narrowband solid state vuv coherent source for laser cooling of antihydrogen,” *Hyperfine Interactions* **235**, 29 (2015).
- [24] G Gabrielse, B Glowacz, D Grzonka, CD Hamley, EA Hessels, N Jones, G Khatri, SA Lee, C Meisenhelder, T Morrison, *et al.*, “Lyman- α source for laser cooling antihydrogen,” *Opt. Lett.* **43**, 2905 (2018).
- [25] EL Surkov, JTM Walraven, and GV Shlyapnikov, “Collisionless motion of neutral particles in magnetostatic traps,” *Phys. Rev. A* **49**, 4778 (1994).
- [26] M. Zhong, J. Fajans, and A.F. Zukor, “Axial to transverse energy mixing dynamics in octupole-based magnetostatic antihydrogen traps,” *New J. Phys.* **20**, 053003 (2018).
- [27] C Ø Rasmussen, N Madsen, and F Robicheaux, “Aspects of 1s-2s spectroscopy of trapped antihydrogen atoms,” *J. Phys. B* **50**, 184002 (2017).
- [28] Claude Cohen-Tannoudji, Jacques Dupont-Roc, and Gilbert Grynberg, *Atom-photon interactions: basic processes and applications* (John Wiley & Sons, 1998).
- [29] Christopher J Foot, *Atomic Physics* (Oxford University Press, 2005).
- [30] “Data for: Simulated optical molasses cooling of trapped antihydrogen,” a link to the data used in the figures will be provided here once the refereeing process is complete and the figures are in final form.